Novel Fe(II) Spin Crossover Complexes Involving Chalcogen-bond and π-Stacking Interactions with a Paramagnetic and Nonmagnetic M(dmit)₂ Anion (M = Ni, Au; dmit = 4,5-dithiolato-1,3-dithiole-2-thione)

Journal Name

ARTICLE

Novel Fe(II) Spin Crossover Complexes Involving Chalcogen-bond and π-Stacking Interactions with a Paramagnetic and Nonmagnetic M(dmit)₂ Anion (M = Ni, Au; dmit = 4,5-dithiolato-1,3-dithiole-2-thione)

Mitsunobu Okai,[a] Kazuyuki Takahashi,*[a] Takahiro Sakurai,[b] Hitoshi Ohta,[c] Takashi Yamamoto,[d] and Yasuaki Einaga[d]

To introduce both an inter-sulphur atom and π-stacking interaction between a spin crossover (SCO) cation and paramagnetic anion, we designed and synthesised two novel Fe(II) SCO compounds involving a terpyridine-type thiazole containing ligand with the paramagnetic Ni(dmit)₂ and nonmagnetic Au(dmit)₂ anion (dmit = 4,5-dithiolato-1,3-dithiole-2-thione). The temperature variations of magnetic susceptibility and Mössbauer spectroscopy revealed that both complexes exhibited an almost complete SCO conversion, and moreover, the Ni(dmit)₂ anion was in a paramagnetic state down to 2 K. The crystal structures for the Ni(dmit)₂ complex at 213 and 400 K indicated that the chalcogen-bond and π-stacking interaction would be enhanced by the electrostatic interaction between the cation and anion, preventing the π-radicals from dimerising. The light-induced excited spin state trapping effect was observed at 5 K.

Introduction

A spin crossover (SCO) phenomenon between a low-spin (LS) and high-spin (HS) state in a transition metal coordination compound is one of molecular switching phenomena induced by temperature, pressure, and light. Since it accompanies changes in not only a magnetic property but also an electronic property, numerous endeavours to utilize the SCO compound itself as a magnetic memory or display device have been examined.[1] In addition, there have been growing interests in the application of the SCO compound as a switching unit to control or tune electronic properties. However, clear correlations between the SCO transition and change in conductivity,[2] magnetism,[3] and optical property[4] have been rarely reported.

Recently we reported an Fe(III) SCO paramagnet where the SCO transition was coupled to a spin-Peierls-like singlet formation of paramagnetic Ni(dmit)₂ anions (dmit = 4,5-dithiolato-1,3-dithiole-2-thione).[3d] Halogen bond interactions between the iodine atom of an SCO cation and the sulphur atom of a paramagnetic anion played a key role in this correlated magnetic transition. As compared with analogous spin-singlet SCO compounds,[5] the cation···anion interaction prevented the paramagnetic Ni(dmit)₂ anions from forming the singlet dimer to stabilise the paramagnetic state in the high temperature phase. This implies that the appropriate introduction of a strong intermolecular interaction into molecular magnetic materials could control the molecular arrangement as well as the spin state.

Ohkoshi and co-workers recently reported the photo-induced ferrimagnetism in an SCO coordination polymer using a cyano-bridged assembly from Fe(II) ions and octacyanoniobate anions with organic co-ligands.[3b] This compound contained an LS Fe(II) ion ($S = 0$) and paramagnetic octacyanoniobate anion ($S = 1/2$) in the low temperature phase. The light-induced excited spin state trapping (LIESST) effect led the paramagnetic compound to a bulk ferrimagnet where the photo-induced HS Fe(II) ion ($S = 2$) was antiferromagnetically coupled to the paramagnetic octacyanoniobate anion ($S = 1/2$). This result encouraged us to develop a similar magnetic SCO compound based on a discrete molecular system, because this would provide valuable information to control a variety of electronic functionalities in common molecular materials.

For a first step to realise the photo-induced magnetic coupling between a discrete SCO cation and paramagnetic anion, we focused on a mononuclear Fe(II) SCO compound and inter-sulphur atom interaction with a paramagnetic Ni(dmit)₂ monoanion ($S = 1/2$), because the Fe(II) SCO compound exhibits a nonmagnetic ($S = 0$) to paramagnetic ($S = 2$) conversion and the introduction of an inter-sulphur atom interaction into the Fe(II) compound resulted in an abrupt SCO transition.[6] For an Fe(II) SCO coordination cation whose ligand includes sulphur atoms, a thiazole containing terpyridine-type ligand is expected to introduce both the inter-sulphur atom and π-stacking interactions into an SCO hybrid compound. Among a series of Fe(II) compounds from thiazole containing ligands,[7] we selected [Fe(II)(L)₂] cation (L = 2,6-bis(2-metylthiazol-4-yl)pyridine),[7b] because this cation gave an indication of SCO conversion above room temperature. We herein report the preparation, crystal structures, and magnetic properties of [Fe(L)₂][Ni(dmit)₂]₂ (1) as well as the analogous compound

[Fe(**L**)$_2$][Au(dmit)$_2$]$_2$ (**2**) involving a nonmagnetic anion (Fig. 1). In comparison between the isostructural paramagnetic compound **1** and nonmagnetic one **2**, both compounds exhibited an almost complete LS to HS SCO conversion, and furthermore the Ni(dmit)$_2$ anion in **1** was in the paramagnetic state down to 2 K. The strong intermolecular chalcogen-bond and π-stacking interactions between the cation and anion played a crucial role in this magnetic behaviour. The LIESST experiment for **1** revealed that a photo-induced HS state could be generated at 5 K.
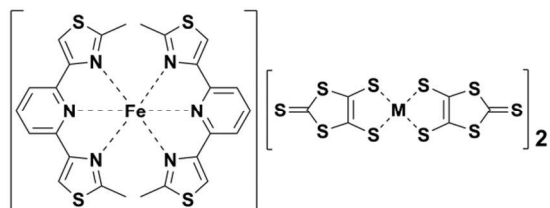
Fig. 1 Molecular structures of [Fe(**L**)$_2$][Ni(dmit)$_2$]$_2$ **1** and [Fe(**L**)$_2$][Au(dmit)$_2$]$_2$ **2**.

Results and discussion

Synthesis

The synthesis of ligand **L** was previously reported by the literature,[7b] but detail procedures and reaction yields were not clearly described. According to the literature,[7b,8] the bromination of 2,6-diacetylpyridine by bromine in CHCl$_3$ or benzene afforded not only the product of 2,6-(dibromoacetyl)pyridine but also many by-products including poly-brominate compounds. The examinations of reaction reagents, solvents, and conditions revealed that using 30%HBr acetic acid solution as a reaction solvent improve the yield of the desired product (37%). The ring formation reaction of the dibromoacetyl compound with thioacetamide in ether did not afford ligand **L**. Thus, the exchange of a reaction solvent to ethanol gave **L** in 84% yield. [Fe(**L**)$_2$](BF$_4$)$_2$ was prepared by the reaction of **L** with Fe(BF$_4$)$_2\cdot$6H$_2$O in ethanol. The metathesis reactions between [Fe(**L**)$_2$](BF$_4$)$_2$ and (TBA)[M(dmit)$_2$] (M = Ni, Au) in acetonitrile gave compounds **1** and **2** as black and dark orange needles, respectively. The compositions for **1** and **2** were determined by microanalysis and crystal structural analyses described below.

Magnetic susceptibilities

The temperature variations of a magnetic susceptibility for **1** and **2** in the temperature range of 2-400 K were measured by using a Quantum Design MPMS magnetometer. The $\chi_M T$ values of **2** below 250 K were almost zero. Since the Au(dmit)$_2$ anion is nonmagnetic, the Fe(**L**)$_2$ cation proved to be in a pure low-spin state. On heating, the $\chi_M T$ values gradually increased and reached to 3.38 cm^3 K mol^{-1} at 400 K, indicating an almost complete SCO conversion occurred. The $\chi_M T$ value for **2** at 400 K was in good agreement with that for typical HS Fe(II) compounds. The $\chi_M T$ value for **1** at 400 K was 4.18 cm^3 K mol^{-1}, which exactly corresponds to the sum of those from an HS Fe(II) cation (S = 2) and two paramagnetic Ni(dmit)$_2$ anions (S = 1/2). On lowering temperatures, the $\chi_M T$ values gradually decreased and reached to 0.86 cm^3 K mol^{-1} at 250 K, suggesting the Fe(II) cation exhibited a gradual SCO transition. However, the spin states for both the Fe(II) cation and paramagnetic

Ni(dmit)$_2$ anion were still unclear. Further cooling, the $\chi_M T$ values for **1** were almost constant in the temperature range of 50-200 K, and then gradually decreased below 50 K. The decrease in $\chi_M T$ might originate from either the SCO conversion of residual HS Fe(II) species or the antiferromagnetic interaction between paramagnetic anions. The field dependence of magnetizations for **1** at 1.9 K is shown in the inset of Fig. 2. The magnetization curve was not well fitted by Brillouin function, but a saturated magnetic moment of 1.9 μ_B corresponds to that of two paramagnetic anions with S = 1/2, suggesting that the decrease in the $\chi_M T$ below 50 K was attributed to the antiferromagnetic interaction. As the magnetic susceptibility curve below 50 K was fitted by the Curie-Weiss law, the fit parameters are C = 0.854 cm^3 K mol^{-1}, θ = −10.4 K.
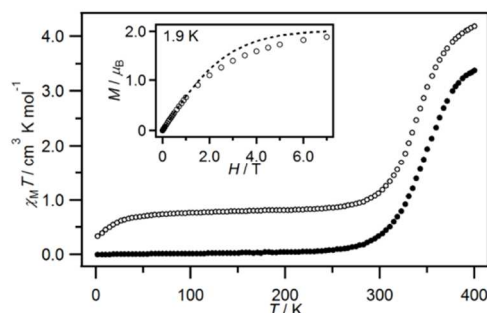
Fig. 2 The $\chi_M T$ versus T plots for **1** (open circles) and **2** (filled circles). Inset shows the magnetic moments of **1** (open circles) and theoretical curve calculated for S = 1/2 $\times$ 2 (broken line) at 1.9 K.

Mössbauer spectra

To confirm the spin state of the Fe(II) ion in **1**, the temperature variations of a Mössbauer spectrum for **1** were recorded at 8.6, 100, 200, 293, 330, 350 K (Fig. 3). The isomer shift (IS) and quadrupole splitting (QS) at each temperature are listed in Table 1. Only one symmetric quadrupole doublet spectrum was observed below 200 K. No difference in the spectrum between 8.6 and 200 K clearly indicated that the decrease in the $\chi_M T$ in the temperature range of 2 - 50 K was not attributed to the SCO conversion. Furthermore, the doublet spectrum above 293 K was transformed to the asymmetric one and shifted to the higher velocities as increasing temperatures. This suggests that the SCO conversion occurred above 293 K. These observations are in good agreement of the magnetic susceptibility data. There was no additional component of each spectrum, because the exchange rate between the HS and LS state was faster than the time scale of a Mössbauer spectrum. A spectrum for **2** at 8.9 K was also composed of one symmetric doublet whose IS and QS were 0.309(6) and 1.074(11) mm s^{-1}, respectively. These parameters were consistent with those for **1** at 8.6 K. This reveals that compounds **1** and **2** prove to be in a pure LS state below 200 K.

Table 1 Temperature variations of Mössbauer parameters for **1** and **2**.

Compound	Temperature / K	IS [1] / mm s^{-1}	QS [2] / mm s^{-1}
1	8.6	0.3189(15)	1.056(3)
	100	0.3202(6)	1.0649(11)
	200	0.2962(10)	1.0772(17)
	293	0.2806(4)	1.1123(8)
	330	0.3952(9)	1.1387(17)
	350	0.557(2)	1.166(4)
2	8.9	0.309(6)	1.074(11)

[1] Isomer shift. [2] Quadrupole splitting.
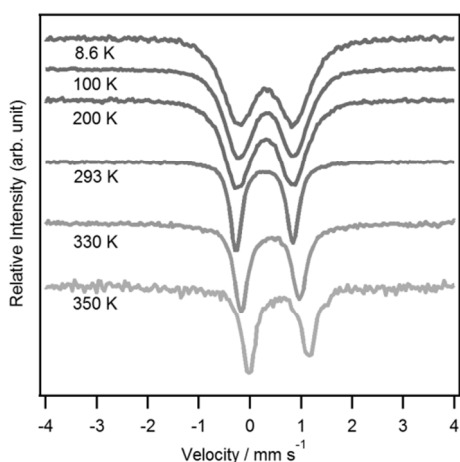
Fig. 3 Mössbauer spectra for **1** at 8.6, 100, 200, 293, 330, and 350 K.

Crystal structural analyses for 1 and 2

The X-ray crystal structural analyses for **1** at 213 and 400 K and for **2** at 213 K were performed by using a Bruker AXS APEX2 ULTRA system. The crystal data for **1** and **2** are listed in Table 2. All the crystal structures for **1** and **2** were isostructural and belonged to monoclinic system with $C2/c$. The asymmetric unit contained one Fe(II) cation, one M(dmit)$_2$ anion, and two half M(dmit)$_2$ anions. The coordination bond lengths and the sums of bite angles derived from 90 ° in the coordination sphere of the Fe(II) cation are listed in Table 3. The bond lengths and Σ value of **1** at 213 K were very similar to those of **2** at 213 K, indicating that both complexes were in the low-spin state. This observation supports that the Ni(dmit)$_2$ anion in **1** was in the paramagnetic state at 213 K. The bond lengths were more than 0.16 Å longer and the Σ value was 46 ° larger in **1** at 400 K, suggesting that compound **1** was in the HS state due to the SCO conversion. The structural changes in **1** were consistent with the magnetic susceptibility data.

The molecular arrangement for compound **1** at 213 K is depicted in Fig. 5. The S···S distances are listed in Table 4. Half independent anions (anion A and B) alternately arranged along the *b* axis, to construct a one-dimensional (1D) uniform zigzag molecular array (Fig. 5a). Two short S···S contacts within the 1D array were 3.456 and 3.536 Å. One independent Ni(dmit)$_2$ anion (anion C) formed a π-dimer in a face-to-face manner. Although the mean π-plane distance was 3.488 Å, there was no short S···S contact within the dimer, because each anion was largely shifted along the molecular long axis as shown in Fig. 5b. The π-ligand of the Fe(II) cation interacted with the Ni(dmit)$_2$ dimer, affording the alternate arrangement of the

Fe(II) cation and anion C along the *b* direction. The mean π-stacking distances between the thiazole and anion C were 3.410 Å for thiazole A and 3.322 Å for thiazole B, respectively. As shown in Fig. 5c, many short S···S contacts between the Fe(II) cation and Ni(dmit)$_2$ anions were found. It should be noted that the remarkable short S···S contact between the S2 atom of the cation and S8 atom of the anion A in the 1D array was found to be 3.282 Å. The C12-S2···S8 angle where the C12 atom was on the thiazole ring was 169.48 °, suggesting the existence of a chalcogen-bond interaction where the S atom of an Ni(dmit)$_2$ anion nucleophilically interacted with the σ-hole of a thiazole ligand.[11] The molecular arrangement comprised a number of the cation···anion interactions including π-stacking and inter-sulphur atom interactions, to construct a two-dimensional (2D) layer parallel to the *ab* plane (Fig. 5d). There were the short S···S contacts between the S12 atoms in one 2D layer and the S15 atoms in the nearest neighbouring layers.

Table 2 Crystallographic data for **1** and **2**.

Compound	1		2
Temperature / K	213	400	213
Empirical formula	C$_{38}$H$_{22}$N$_6$S$_{24}$FeNi$_2$		C$_{38}$H$_{22}$N$_6$S$_{24}$FeAu$_2$
Formula weight	1505.41		1781.84
Dimension	0.4×0.06×0.01	0.4×0.03×0.01	0.13×0.06×0.01
Crystal system	Monoclinic	Monoclinic	Monoclinic
Space group	$C2/c$	$C2/c$	$C2/c$
a / Å	22.776(3)	24.117(5)	22.892(2)
b / Å	13.616(2)	13.501(3)	13.6036(14)
c / Å	35.453(5)	35.467(7)	35.684(4)
α / °	90	90	90
β / °	97.2283(19)	97.911(3)	96.3714(14)
γ / °	90	90	90
V / Å^3	10907(3)	11438(4)	11043.8(19)
Z	8	8	8
No. Reflections	29254	26076	26220
No. Observations	11534	9735	9756
$(I > 2\sigma(I))$	(9113)	(4512)	(7840)
No. Variables	647	647	647
R_1 [1] $(I > 2\sigma(I))$	0.0353	0.0783	0.0354
R_1 [1] (all data)	0.0513	0.1877	0.0515
wR_2 [2] $(I > 2\sigma(I))$	0.0762	0.1440	0.0743
wR_2 [2] (all data)	0.0824	0.1838	0.0801
Goodness of fit	1.035	1.048	1.032

[1] $R_1 = \Sigma||F_o| - |F_c||/\Sigma|F_o|$. [2] w$R_2 = [\Sigma w(F_o^2 - F_c^2)^2/\Sigma w(F_o^2)^2]^{1/2}$.
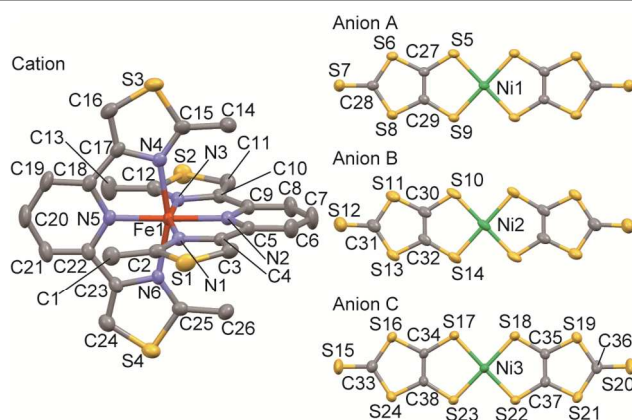
Fig. 4 ORTEP diagrams (50% probability) with atomic numbering schemes for **1** at 213 K. Hydrogen atoms are omitted for clarity.
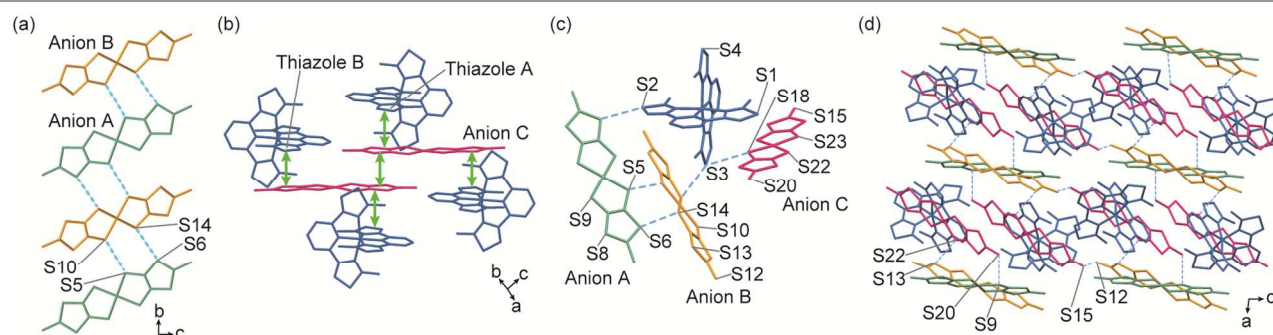
Fig. 5 Crystal structures of **1** with selected atomic numbering schemes at 213 K (blue broken lines indicate short S···S contacts). Hydrogen atoms are omitted for clarity. (a) A 1D zigzag array of Ni(dmit)$_2$ anions. (b) A π-stacking arrangement of the Ni(dmit)$_2$ anions C and Fe(**L**)$_2$ cations (green double-headed arrows indicate the π–stacking interaction). (c) A molecular arrangement between the cation and anion. (d) A layered packing diagram projected along the *b* axis

Table 3 Selected bond lengths (Å) and angles (°) of **1** and **2**.

Compound	**1**		**2**
Temperature / K	213	400	213
Spin state	LS	HS	LS
Fe1–N1	2.023(2)	2.186(8)	2.014(5)
Fe1–N2	1.915(2)	2.096(8)	1.918(4)
Fe1–N3	2.021(2)	2.194(9)	2.013(5)
Fe1–N4	2.017(2)	2.190(7)	2.017(5)
Fe1–N5	1.917(2)	2.101(7)	1.917(4)
Fe1–N6	2.016(2)	2.197(7)	2.021(5)
Σ[1]	78.01	124.1	78.62

[1] Σ is the sum of the deviations of the bite angles from 90 °.

Table 4 Selected inter-atom and inter-plane distances (Å) for **1** and **2** within the 1D layer.

Compound		**1**		**2**
Temperature		213 K	400 K	213 K
Inter-atom				
Anion A	Anion B			
S5	S10	3.4565(12)	3.518(5)	3.377(2)
S6	S14	3.5360(12)	3.550(6)	3.546(2)
Anion A	Anion C			
S9	S20	3.5290(13)	3.578(4)	3.590(3)
Anion B	Anion C			
S12	S15[1]	3.5612(17)	3.558(9)	3.589(3)
S13	S22	3.4813(11)	3.612(5)	3.463(2)
S13	S23	3.6269(11)	4.004(4)	3.592(2)
Cation	Anion			
S2	S8 (A)	3.2821(11)	3.293(5)	3.294(2)
S3	S14 (B)	3.5220(11)	3.699(5)	3.569(2)
S3	S18 (C)	3.4857(11)	3.667(4)	3.430(2)
Inter-plane				
Anion C	Anion C	3.488	3.499	3.507
Thiazole A	Anion C	3.410	3.439	3.343
Thiazole B	Anion C	3.322	3.480	3.322

[1] The anions were involved in the neighbouring 2D layers.

The molecular arrangement of **2** at 213 K was quite similar to that of **1** at 213 K. There was no remarkable difference in the intermolecular distances. This implies that whether a paramagnetic or nonmagnetic anion did not affect the crystal structures.

Only the *a* axis expanded a length of 1.34 Å in **1** at 400 K. This suggests that the 1D zigzag array and molecular arrangement between the 2D layers unchanged, whereas the alternate cation-anion molecular arrangement changed from

that at 213 K. In fact, the S···S distances between anion A and C, and between anion B and C within the 2D layer lengthened at 400 K. In addition, the S···S distances between the cation and anion B and between the cation and anion C were 0.17 and 0.18 Å longer, respectively. The mean π-stacking distance between the thiazole B and anion C was also 0.16 Å longer. These structural variations attributed to the shift of each anion C to the opposite direction along the molecular long axis. On the other hand, there were no remarkable variations of the short S···S distances in the 1D zigzag array and between the 2D layers. It should be noted that the subtraction of the mean π-stacking distance between the thiazole A and anion C was less than 0.03 Å and that of the S···S distance in the chalcogen bond interaction between the cation and anion A was only 0.01 Å.

Table 5. Transfer integrals (meV) between Ni(dmit)$_2$ anions of **1**.

Compound		**1**	
Temperature / K		213	400
Intralayer			
Anion A	Anion B	30.9	26.4
Anion A	Anion C	-27.4	-30.9
Anion A	Anion C[1]	8.0	4.7
Anion B	Anion C	-7.3	-3.6
Anion C	Anion C[1]	16.0	1.5
Interlayer			
Anion A	Anion C[1]	-13.3	-12.8
Anion B	Anion C	-7.2	1.3

[1] No short S···S contact for the neighbouring anion.

Transfer integrals between the Ni(dmit)$_2$ anions

The exchange coupling energy *J* is proportional to the square of a transfer integral. To estimate the magnetic exchange interaction between neighbouring Ni(dmit)$_2$ anions, transfer integrals were calculated based on the extended Hückel method and listed in Table 5. The transfer integrals in the 1D array and between the dimer for **1** at 213 K were 30.9 and 16.0 meV, respectively. The other transfer integrals were less than 30 meV. Since the transfer integral in the paramagnetic Ni(dmit)$_2$ compound reported previously was 89.6 meV,[12] the Ni(dmit)$_2$ anion in **1** at 213 K is in the paramagnetic state. This is in good agreement with the description in the magnetic susceptibilities and Mössbauer spectra sections. Most of the transfer integrals at 400 K were smaller than those at 213 K.

Conducting properties

Although electrical conductivity for **1** at room temperature was measured by a conventional four-probe method, compound **1** was an insulator, which is consistent with the isolated paramagnetic behaviour and small transfer integrals between the anions.

Correlation between structures and magnetic properties

The magnetic behaviour and crystal structures revealed that compound **1** was the Fe(II) SCO paramagnet possessing the equally spaced 1D chains with $S = 1/2$. In general, the 1D chain compound with $S = 1/2$ undergoes a spin-singlet formation transition at low temperature. However, the magnetic susceptibility data imply that the magnetic transition was absent for **1**. This suggests that some intermolecular interactions prevent the paramagnetic ions with $S = 1/2$ from the spin-singlet formation.

The temperature dependence of the crystal structures for **1** indicated that both the chalcogen-bond interaction between the cation and anion and the π-stacking interaction between the π-ligand of the cation and anion C were unchanged before and after the SCO conversion. Since the SCO transition accompanies the changes in the coordination bond lengths and angles which lead to the changes in the intermolecular molecular arrangement, the unchanged interactions are thought to be the dominant interactions to construct the crystal structure of **1**.

The chalcogen-bond interaction is highly directional, because the σ-hole exists around the outer space of a sulphur atom approximately along the extension of a covalent bond to sulphur.[11] The substitution with an electron-withdrawing group or the cationisation of a neutral molecule enhances the positive portion of the σ-hole to strengthen the chalcogen-bond interaction. In the present case, the coordination with an Fe(II) ion was thought to enhance the chalcogen-bond interaction.

There were two kinds of the π-staking interactions between the cation and anion C in **1**. However, the SCO conversion unchanged one π-staking interaction, whereas changed the other one. As compared with the distances between the Fe and Ni atoms at 213 K, the unchanged interaction has a shorter distance of 6.212 Å, whereas the changed interaction has a longer one of 7.642 Å. This implies that the electrostatic interaction may play a key role in the strong π-stacking interaction.

Therefore, both the chalcogen-bond and π-stacking interactions were enhanced by the metal coordination effect. Despite many S⋯S short contacts between the Ni(dmit)$_2$ anions, the transfer integrals were extremely small. This suggests that the chalcogen-bond and π-stacking interactions between the cation and anion governed the arrangement of the Ni(dmit)$_2$ anions, leading to the stabilisation of the paramagnetic state for the Ni(dmit)$_2$ anion.

Photo response of 1

The photo-induced experiment on $\chi_M T$ for **1** was carried out on a ground sample (Fig. 6). On illumination with a YAG laser (532 nm) at 5 K, the $\chi_M T$ value of **1** gradually increased, suggesting that the metastable HS state could be trapped. After irradiation for 3 hours, $\chi_M T$ reached a value of 0.43 cm^3 K mol^{-1}, indicating the low conversion of a LS into the metastable HS state. On heating, the value of $\chi_M T$ gradually increased up to 40 K, and then completely relaxed to the ground LS state at 70 K.

In the cooling process the $\chi_M T$ values traced the original ones, indicating that the photo-induced change in $\chi_M T$ was reversible. On the other hand, no increase in $\chi_M T$ was observed on irradiation with 830 nm. This means that the photo-induced increase in $\chi_M T$ results from a photo process not a thermal one. There are two possibilities for the small change in $\chi_M T$. One reason is the absorption of light by a sample, another one is the antiferromagnetic coupling between the photo-induced HS Fe(II) cations and paramagnetic anions. To clarify the spin state of the Fe(II) ion, Mössbauer spectrum for **1** was measured before and after photo irradiation. Unfortunately the difference in the spectra after the photo illumination was not clearly detected. Further experiments such as magnetization measurements at very low temperatures after photo irradiation will be needed to clarify the photo-response to the magnetic exchange interaction between the cation and anion.
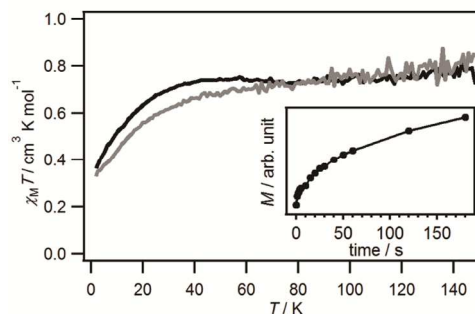
Fig. 6 $\chi_M T$ versus T plots for **1** before (gray) and after illumination with 532 nm (black) at 5 K. Inset shows the time dependence of magnetizations during irradiation with 532 nm.

Conclusion

Two novel Fe(II) SCO compounds involving the thiazole containing ligand with the paramagnetic Ni(dmit)$_2$ and nonmagnetic Au(dmit)$_2$ anion exhibited the almost complete SCO conversion and, furthermore, it was successful to stabilise the paramagnetic state for the Ni(dmit)$_2$ anion down to 2 K due to the strong chalcogen-bond and π-stacking interaction. Compound **1** is the first Fe(II) SCO hybrid compound containing the paramagnetic π-radical absent from a spin-singlet π-dimer formation. The enhancement of the chalcogen-bond and π-stacking interactions by the metal coordination effect has never been clearly described. This effect would afford versatile tools for the crystal engineering in functional transition metal coordination materials. Although the LIESST effect on **1** was observed, the exchange coupling between the HS Fe(II) ion and paramagnetic Ni(dmit)$_2$ anion was not clearly evidenced. If the effective overlap of molecular orbitals between the π-ligand in the SCO cation and π-radical anion can be introduced into an SCO hybrid molecular system, it may be possible to realise the magnetic exchange coupling between the SCO cation and paramagnetic π-anion. Further molecular designs to achieve this goal are currently in progress.

Experimental

Synthesis

All reagents were obtained from commercial sources and were used without further purification. $(TBA)[Ni(dmit)_2]^9$ and $(TBA)[Au(dmit)_2]^{10}$ were prepared according to the literature.

Synthesis of 2,6-bis(bromoacetyl)pyridine

To a solution of 2,6-diacetylpyridine (1 g, 6.13 mmol) in 5 mL of 30%HBr acetic acid solution was added dropwise a solution of bromine (0.7 mL, 13.6 mmol) in the mixed solution of 30%HBr acetic acid (2 mL) and acetic acid (3 mL) at room temperature. After stirring for 4 hours, a saturated aqueous solution of sodium hydrogen sulphite was added, and then neutralised by sodium bicarbonate. The precipitates were filtered, and dried under vacuum. Colourless powder (0.744 g, 37%). ^1H NMR (400MHz, $CDCl_3$) δ 8.33(d, J = 7.8 Hz, 2H), 8.11(t, J = 7.8 Hz, 1H), 4.82(s, 4H) ppm.

Synthesis of 2,6-bis(2-methylthiazol-4-yl)pyridine (L)

To a hot solution of 2,6-bis(bromoacetyl)pyridine (0.740 g, 2.31 mmol) in 9 mL of ethanol was added dropwise a solution of thioacetamide (0.346 g, 4.61 mmol) in 4 mL of ethanol. After heating to reflux, a colourless precipitate appeared. After neutralisation by using a saturated aqueous solution of sodium bicarbonate, the precipitate was filtered, and then dried under vacuum. Ligand **L** (0.527 g, 1.93 mmol) was obtained as a colourless powder in 84% yield. ^1H NMR (400MHz, $CDCl_3$) δ 8.03(s, 2H), 8.02(d, J = 6.8 Hz, 2H), 7.83(t, J = 7.8 Hz, 1H), 2.80(s, 6H) ppm.

Synthesis of [Fe(L)₂](BF₄)₂

To a hot solution of **L** (70.5 mg, 0.258 mmol) in 4 mL of ethanol was added dropwise a solution of $Fe(BF_4)_2 \cdot 6H_2O$ (43.6 mg, 0.129 mmol) in 1.1 mL of ethanol, and then 4 mL of ethanol was added. The reaction mixture was heated under reflux for 30 min, and then cooled to room temperature. The precipitate was filtered and dried in air. $[Fe(\mathbf{L})_2](BF_4)_2$ (90.5 mg, 90%) was obtained as dark red leaflets.

Synthesis of [Fe(L)₂][Ni(dmit)₂]₂ (1)

To a solution of $TBA[Ni(dmit)_2]$ (41.8 mg, 0.060 mmol) in 150 mL of acetonitrile was added in one portion a solution of $[Fe(\mathbf{L})_2](BF_4)_2$ (23.5 mg, 0.030 mmol) in 100 mL of acetonitrile. After being placed overnight, the precipitate was filtered and dried under vacuum. **1** (31.8 mg, 70%) was obtained as black needles. Anal. Calcd. for $C_{38}H_{22}N_6Ni_2FeS_{24}$: C, 30.32; H, 1.47; N, 5.58%. Found: C, 30.20; H, 1.59; N, 5.51%.

Synthesis of [Fe(L)₂][Au(dmit)₂]₂ (2)

To a solution of $TBA[Au(dmit)_2]$ (24.8 mg, 0.030 mmol) in 112.5 mL of acetonitrile was added in one portion a solution of $[Fe(\mathbf{L})_2](BF_4)_2$ (11.7 mg, 0.015 mmol) in 75 mL of acetonitrile. After being placed overnight, the precipitate was filtered and dried under vacuum. **2** (20.1 mg, 75%) was obtained as dark

orange needles. Anal. Calcd. for $C_{38}H_{22}N_6Au_2FeS_{24}$: C, 25.61; H, 1.24; N, 4.72%. Found: C, 25.70; H, 1.29; N, 4.77%.

Magnetic measurements

Variable temperature DC magnetic susceptibilities of a polycrystalline sample (ca. 20 mg) sealed in a gelatine capsule were measured on a Quantum Design MPMS-XL magnetometer under a field of 0.5 T and at a sweep speed of 2 K min^{-1} in the temperature range of 2-300 K. Data were corrected for diamagnetic contributions estimated by Pascal constants.

The photo effect on the magnetization of a sample was measured by using a YAG laser (532 nm, CrystaLaser GCL-100L). The light was guided by a quartz optical fibre into the sample chamber of the magnetometer. The sample was placed between quartz rods and the upper rod was connected with one end of the optical fibre.

Mössbauer spectroscopy

The Mössbauer spectra were recorded on a constant acceleration spectrometer with a source of $^{57}Co/Rh$ in the transmission mode. The measurements were performed with a closed-cycle helium refrigerator (Iwatani Co., Ltd.). The obtained Mössbauer spectra were fitted with symmetric Lorentzian doublets by the least squares fitting program (MossWinn).

X-ray single crystal structural analyses

Data Collection, Structure Solution, and Structure Refinement. A needle crystal was mounted in a polyimide loop. A nitrogen gas flow temperature controller was used for the temperature variable measurements. All data were collected on a Bruker APEX II CCD area detector with monochromated Mo-$K\alpha$ radiation generated by a Bruker Turbo X-ray Source coupled with Helios multilayer optics. All data collections and calculations were performed using the APEX2 crystallographic software package (Bruker AXS). The data were collected to a maximum 2θ value of 55.0º. A total of 720 oscillation images were collected. The APEX II program was used to determine the unit cell parameters and for data collection. Data were integrated by using SAINT. Numerical absorption correction was applied by using SADABS. The structures at all temperatures were solved by direct methods and refined by full-matrix least-squares methods based on F^2 by using the SHELXTL program. All non-hydrogen atoms were refined anisotropically. Hydrogen atoms were generated by calculation and refined using the riding model. The attenuation of the diffracted X-rays probably due to thermal molecular motion effects led to the Alert level B in the checkCIF report.

Transfer integral calculations

The transfer integrals (t) were calculated by the extended Hückel molecular orbital calculation method by using the lowest unoccupied molecular orbital (LUMO) of $Ni(dmit)_2$ as the basis function within the tight-binding approximation.[13] The semiempirical parameters of Ni, S, and C for Slater-type atomic

orbitals were taken from the literature.[14,15] The t between each pair of molecules was assumed to be proportional to the overlap integral (S), $t = ES$, where E is a constant value of -10.0 eV.

Acknowledgements

Notes and references

[a] Department of Chemistry, Graduate School of Science, Kobe University, Kobe, Hyogo 657-8501, Japan. E-mail: ktaka@crystal.kobe-u.ac.jp

[b] Center for Supports to Research and Education Activities, Kobe University, Kobe, Hyogo 657-8501, Japan

[c] Molecular Photoscience Research Center, Kobe University, Kobe, Hyogo 657-8501, Japan

[d] Department of Chemistry, Keio University, Yokohama, Kanagawa 223-8522, Japan

† Crystallographic data reported in this manuscript have been deposited with Cambridge Crystallographic Data Centre as supplementary publication no. CCDC 1056374-1056376. Copies of the data can be obtained free of charge via www.ccdc.cam.ac.uk/conts/retrieving.html (or from the Cambridge Crystallographic Data Centre, 12, Union Road, Cambridge, CB2 1EZ, UK; fax: +44 1223 336033; or deposit@ccdc.cam.ac.uk).

1   Recent review for SCO applications; A. Bousseksou, G. Molnár, L. Salmon, and W. Nicolazzi, *Chem. Soc. Rev.*, 2011, **40**, 3313.

2   (a) K. Takahashi, H.-B. Cui, Y. Okano, H. Kobayashi, Y. Einaga, and O. Sato, *Inorg. Chem.*, 2006, **45**, 5739; (b) K. Takahashi, H.-B. Cui, Y. Okano, H. Kobayashi, H. Mori, H. Tajima, Y. Einaga, and O. Sato, *J. Am. Chem. Soc.*, 2008, **130**, 6688; (c) B. Djukic and M. T. Lemaire, *Inorg. Chem.*, 2009, **48**, 10489; (d) M. Nihei, N Takahashi, H. Nishikawa, and H. Oshio, *Dalton Trans.*, 2011, **40**, 2154; (e) H. Phan, S. M. Benjamin, E. Steven, J. S. Brooks, and M. Shatruk, *Angew. Chem. Int. Ed.*, 2015, **54**, 823.

3   (a) M. Nihei, H. Tahira, N. Takahashi, Y. Otake, Y. Yamamura, K. Saito, and H Oshio, *J. Am. Chem. Soc.*, 2010, **132**, 3553; (b) S. Ohkoshi, K. Imoto, Y. Tsunobuchi, S. Takano, and H. Tokoro, *Nat. Chem.*, 2011, **3**, 564; (c) R. Ababei, C. Pichon, O. Roubeau, Y.-G. Li, N. Bréfuel, L. Buisson, P. Guionneau, C. Mathonière, and R. Clérac, *J. Am. Chem. Soc.*, 2013, **135**, 14840; (d) K. Fukuroi, K. Takahashi, T. Mochida, T. Sakurai, H. Ohta, T. Yamamoto, Y. Einaga, and H. Mori, *Angew. Chem. Int. Ed.*, 2014, **53**, 1983.

4   (a) S. Ohkoshi, S. Takano, K. Imoto, M. Yoshikiyo, A. Namai, and H. Tokoro, *Nat. Photonics*, 2014, **8**, 66; (b) C. F. Wang, R.-F. Li, X.-Y. Chen, R.-J. Wei, L.-S. Zheng, and J. Tao, *Angew. Chem. Int. Ed.*, 2015, **54**, 1574.

5   (a) K. Takahashi, H.-B. Cui, H. Kobayashi, Y. Einaga, and O. Sato, *Chem. Lett.*, 2005, **34**, 1240; (b) K. Takahashi, H. Mori, H. Kobayashi, and O. Sato, *Polyhedron*, 2009, **28**, 1776.

6   K. Takahashi, T. Kawakami, Z.-Z. Gu, Y. Einaga, A. Fujishima, and O. Sato, *Chem. Commun*, 2003, 2374.

7   (a) S. E. Livingstone and J. D. Nolan, *Dalton Trans.*, 1972, 218.; (b) A. T. Baker and H. A. Goodwin, *Aust. J. Chem.*, 1984, **37**, 2431; (c) A. T. Baker, P. Singh, and V. Vignevich, *Aust. J. Chem.*, 1991, **44**, 1041.

8   L. W. Deady and M. S. Stanborough, *Aust. J. Chem.*, 1981, **34**, 1295.

9   G. Steimecke, H.-J. Sieler, R. Kirmse, and E. Hoyer, *Phosphorous, Sulfur Relat. Elem.*, 1979, **7**, 49.

10 R. Kirmse, J. Stach, W. Dietzsch, G. Steimecke, and E. Hoyer, *Inorg. Chem.*, 1980, **19**, 2679.

11 (a) J. S. Murray, P. Lane, and P. Politzer, *Int. J. Quantum Chem.*, 2008, **108**, 2770; (b) T. Kusamoto, H. Yamamoto, and R. Kato, *Cryst. Growth Des.*, 2013, **13**, 4533.

12 T. Akutagawa and T. Nakamura, *Coord. Chem. Rev.*, 2002, **226**, 3.

13 T. Mori, A. Kobayashi, Y. Sasaki, H. Kobayashi, G. Saito, and H. Inokuchi, *Bull. Chem. Soc. Jpn.*, 1984, **57**, 627.

14 R. H. Summerville, R. Hoffmann, *J. Am. Chem. Soc.*, 1976, **98**, 7240.

15 H. Kobayashi, H. Tomita, T. Naito, A. Kobayashi, F. Sakai, T. Watanabe, and P. Cassoux, *J. Am. Chem. Soc.*, 1996, **118**, 368.

TOC

A novel Fe(II) complex with a π-radical anion exhibited a complete spin crossover transition with a stable paramagnetic state due to strong chalcogen-bond and π-stacking interactions.